

# Journal of Biomedical Optics

[SPIEDigitalLibrary.org/jbo](http://SPIEDigitalLibrary.org/jbo)

## **Continuous haematic pH monitoring in extracorporeal circulation using a disposable fluorescence sensing element**

Luca Ferrari  
Luigi Rovati  
Paola Fabbri  
Francesco Pilati



**SPIE**

# Continuous haematic pH monitoring in extracorporeal circulation using a disposable fluorescence sensing element

Luca Ferrari, Luigi Rovati, Paola Fabbri, and Francesco Pilati

University of Modena and Reggio Emilia, Department of Engineering Enzo Ferrari, Strada Vignolese 905, I-41125, Modena, Italy

**Abstract.** During extracorporeal circulation (ECC), blood is periodically sampled and analyzed to maintain the blood-gas status of the patient within acceptable limits. This protocol has well-known drawbacks that may be overcome by continuous monitoring. We present the characterization of a new pH sensor for continuous monitoring in ECC. This monitoring device includes a disposable fluorescence-sensing element directly in contact with the blood, whose fluorescence intensity is strictly related to the pH of the blood. *In vitro* experiments show no significant difference between the blood gas analyzer values and the sensor readings; after proper calibration, it gives a correlation of  $R > 0.9887$ , and measuring errors were lower than the 3% of the pH range of interest (RoI) with respect to a commercial blood gas analyzer. This performance has been confirmed also by simulating a moderate hypothermia condition, i.e., blood temperature 32°C, frequently used in cardiac surgery. In *ex vivo* experiments, performed with animal models, the sensor is continuously operated in an extracorporeal undiluted blood stream for a maximum of 11 h. It gives a correlation of  $R > 0.9431$ , and a measuring error lower than the 3% of the pH RoI with respect to laboratory techniques. © 2013 Society of Photo-Optical Instrumentation Engineers (SPIE) [DOI: 10.1117/1.JBO.18.2.027002]

Keywords: biomedical optics; fluorescence; optical systems; polymer.

Paper 12637 received Sep. 25, 2012; revised manuscript received Dec. 18, 2012; accepted for publication Dec. 20, 2012; published online Feb. 1, 2013.

## 1 Introduction

Extracorporeal circulation (ECC) is mainly applied in cardiopulmonary bypass, extracorporeal membrane oxygenation, and hemodialysis. Usually, during ECC, blood samples are drawn intermittently and analyzed by a blood gas analyzer. Major problems associated with this intermittent sampling are: (1) high cost of the blood gas analyzer and required reagents thus analyses are often performed only after adverse events; (2) there is a risk of blood loss and infection; and (3) therapeutic response can only be made after a delay. Considerable spontaneous variability in blood gases and other quickly changing analytes that occur during ECC require clinical decisions made on the basis of trends observed with continuous monitoring. Usually, the information of interest includes hemoglobin saturation, hematocrit, blood gases ( $O_2$ ,  $CO_2$ ), pH, electrolytes ( $Na^+$ ,  $K^+$ ,  $Ca^{2+}$ ,  $Cl_2$ ), certain metabolites (glucose, lactate, urea, creatinine), and physical measurands (temperature, pressure, flow). Several sensors capable of continuously monitoring these parameters have been so far proposed.<sup>1,2</sup> Nevertheless, despite tremendous technological efforts, the proposed technologies are not yet sufficiently reliable and economic to be used routinely in ECC and frequent intermittent measurements made by a blood gas analyzer near the bedside are still the standard practice. Since ECC through flow cuvettes offers a perfect optical access to circulating blood, several optical approaches have been considered,<sup>3-9</sup> and few commercial optical continuous intravascular blood gas monitoring devices are nowadays available: Paratrend 7+ (PT7+) for adults and Neotrend (NT) for newborns, both based on optical absorption and reflectance methods.<sup>10</sup> However, they

have been rarely used due to their instability and inaccuracies.<sup>11,12</sup> In ECC, haematic pH is one of the most interesting blood parameter. pH, in fact, is strongly related to the functioning of important organs such as lung, heart, liver, and kidney. The haematic pH, in healthy human beings, is always between 7.30 and 7.45, thanks to the bicarbonate buffering system. Nevertheless, a little variation of pH can produce great damages for the body. Many efforts have been spent on the development of pH sensors to be applied in ECC. Continuous blood pH measurements can be made potentiometrically via ion-selective electrodes or transistors. These devices are based on ionophores that may leach out of the ion-selective membranes, thus resulting in lower stability and short lifetime.<sup>13</sup> This stability issue limits the use of ion-selective electrodes or transistors in ECC. Attempts to use electrochemical sensors were hampered by protein deposition on the active or reference electrodes that prevents their use unless regular recalibration.<sup>2</sup> While promising, none of these methods are suitable for continuous monitoring in ECC. As for the other quantities of interest in ECC, there has been considerable interest in optical methods of determining pH. In literature, proposed pH sensors are mainly based on the immobilization of pH-sensitive absorbing dyes<sup>14-16</sup> or fluorophores<sup>17,18</sup> on a solid substrate. One of the major limitation of such a sensor is still the dye leaching into blood,<sup>19</sup> that, besides problems related to signal stability, can represent a risk for the patient, if the dye is toxic. A further disadvantage of the sensors based on fluorophores is their propensity for photobleaching.<sup>19</sup> For all these reasons, while many pH optical sensors have been proposed for continuous pH monitoring, *in vivo* results have not been reported so far. In the present study, we use a novel pH sensor based on a polymeric sensing substrate, directly in contact with the blood, encapsulating the pH-indicator.<sup>20</sup> The

Address all correspondence to: Luca Ferrari, University of Modena and Reggio Emilia, Department of Engineering Enzo Ferrari, Strada Vignolese 905, I-41125, Modena, Italy. Tel: +39 059 205 6109; Fax: +39 059 205 6129; E-mail: [luca.ferrari@unimore.it](mailto:luca.ferrari@unimore.it)

pH-sensitive fluorophore is the fluorescein O-methacrylate 97%, which can be covalently linked to the polymeric sensing element. This sensing approach offers several advantages: (1) simple fabrication and low-cost, thus the sensing element is disposable; (2) thanks to the covalent link, minimal leaching of the fluorophore into the blood; (3) biocompatibility (fluorescein is used in several medical practises, e.g., fluoroangiography); and (4) mechanical robustness. The interrogation optical head was realized using a low-cost light source [light-emitting diode (LED)] and two photodiodes, to monitor both the power emitted by the LED and the fluorescence signal emitted by the sensing element. Fluorophores photobleaching was compensated by proper modulation of the optical source.<sup>21</sup> Whole blood was used in this work to demonstrate the monitoring performances both *in vitro* and *ex vivo* experiments over long periods. In the next section a brief introduction of the principle of measurement is given whereas the optical transducer, flow cuvette and the electronic circuitry are described in the first paragraph of Sec. 3. Sections 3.3, 3.4, and 3.5 deal with the description of the experimental setup and the measurement procedure, while the results of the sensor characterization, both *in vitro* and *ex vivo* are reported in Sec. 4. Finally, conclusions are drawn and discussed in Sec. 5.

## 2 Theoretical Background

The proposed sensing approach consists in the fluorometric determination of pH.<sup>22</sup> Fluorescence measurements of pH are based on the detection of the concentration of the acid and base forms of the fluorophore and are not related to activity of the hydrogen ions as in potentiometric pH determinations. However, the unknown ionic strength of the sample affects the equilibrium constant, and hence the pH calculated from the measured degree of dissociation of the indicator. Thus this approach requires a proper calibration procedure. It is already known that fluorescence intensity of fluorescein molecule is dramatically reduced at acidic pH when excitation is performed at 490 nm.<sup>23</sup> In particular, as discussed in the next section, we deploy the pH-dependency of the emission spectra of the fluorescein O-methacrylate 97%. The response curve of this sensing approach derives from the mass-action law relationship between pH and radiation intensity.<sup>24</sup> Considering the free dye, if the fluorescence intensity of the fully protonated system is  $I_{\min}$  and assuming equal to  $I_{\max}$  the fluorescence contribution of the deprotonated system, the intensity of fluorescence emission  $I_s$  in the presence of the sample under test is then converted to pH, by the relation:<sup>25</sup>

$$\text{pH} = pK_a - \log\left(\frac{\frac{I_{\max} - I_s}{I_o}}{\frac{I_s - I_{\min}}{I_o}}\right) = pK_a - \log\left(\frac{\frac{I_{\max} - I_{\text{ratio}}}{I_o}}{\frac{I_{\text{ratio}} - I_{\min}}{I_o}}\right), \quad (1)$$

where  $pK_a$  is the acid-base constant of the indicator,  $I_o$  is the excitation light intensity, and  $I_{\text{ratio}}$  is equal to  $I_s/I_o$ . It has to be noticed that the parameters  $I_{\text{ratio}} = I_s/I_o$ ,  $I_{\max}/I_o$ , and  $I_{\min}/I_o$  are insensitive to possible small fluctuations of the excitation light intensity. Considering the dye covalently linked to the polymer matrix, Eq. (1) is modified<sup>25,26</sup> and become:

$$\text{pH} = pK_a - b \cdot \log\left(\frac{\frac{I_{\max} - I_{\text{ratio}}}{I_o}}{\frac{I_{\text{ratio}} - I_{\min}}{I_o}}\right), \quad (2)$$

where  $b$  is a numerical coefficient, introduced to determine the slope of the function between  $I_{\max}$  and  $I_{\min}$ . In fact, the chemical and physical properties of the matrix encapsulating the dye (e.g., polarity and viscosity) could affect its sensitivity near the  $pK_a$ , thus having different slopes for the same indicator in different matrices. Rewriting Eq. (2) in terms of  $I_{\text{ratio}}$ , gives the well-known sigmoidal function:<sup>26</sup>

$$\begin{aligned} I_{\text{ratio}} &= \frac{1}{I_o} \cdot \frac{I_{\max} + I_{\min} \cdot 10^{-\left(\frac{\text{pH} - pK_a}{b}\right)}}{1 + 10^{-\left(\frac{\text{pH} - pK_a}{b}\right)}} \\ &= \frac{I_{\min}}{I_o} + \frac{1}{I_o} \cdot \frac{I_{\max} - I_{\min}}{1 + 10^{-\left(\frac{\text{pH} - pK_a}{b}\right)}}. \end{aligned} \quad (3)$$

The pH of blood is related to the constituents of the bicarbonate buffer system by the modified Henderson-Hasselbalch equation:<sup>27</sup>

$$\text{pH}_{\text{blood}} = pK_{a_{\text{H}_2\text{CO}_3}} + \log\left(\frac{[\text{HCO}_3^-]}{[\text{H}_2\text{CO}_3]}\right), \quad (4)$$

where  $pK_{a_{\text{H}_2\text{CO}_3}}$  is the acid dissociation constant of the carbonic acid, which is equal to 6.1,  $[\text{HCO}_3^-]$  is the concentration of bicarbonate in the blood, and  $[\text{H}_2\text{CO}_3]$  is the concentration of carbonic acid in the blood. Considering the partial pressure of carbon dioxide,  $p\text{CO}_2$ , rather than  $[\text{H}_2\text{CO}_3]$ , Eq. (4) can be written as:

$$\text{pH}_{\text{blood}} = 6.1 + \log\left(\frac{[\text{HCO}_3^-]}{0.03 \times p\text{CO}_2}\right). \quad (5)$$

Equation (5) provides a pH value for healthy human beings between 7.30 and 7.45. These pH values are very close to the  $pK_a$  of our sensing membrane, i.e.,  $I_{\text{ratio}} = (I_{\max} + I_{\min})/2I_o$ , thus the argument of the logarithmic function in Eq. (2) is close to one. According to the first-order Taylor polynomial of the logarithmic function, the approximation of Eq. (2) is:

$$\text{pH} = pK_a - 2 \cdot b \cdot \log(e) \cdot \left(\frac{\frac{I_{\max} + I_{\min}}{2I_o} - I_{\text{ratio}}}{I_{\text{ratio}} - \frac{I_{\min}}{I_o}}\right). \quad (6)$$

Since pH values are very close to the  $pK_a$  of our sensing membrane, i.e.,  $I_{\text{ratio}} = (I_{\max} + I_{\min})/2I_o$ , the term

$$\frac{\frac{I_{\max} + I_{\min}}{2I_o} - I_{\text{ratio}}}{I_{\text{ratio}} - \frac{I_{\min}}{I_o}}, \quad (7)$$

is close to zero. According to the first-order Taylor polynomial of the rational function, Eq. (6) can be rewritten as:

$$\text{pH} = \text{p}K_a + 2 \cdot b \cdot \log(e) \cdot \frac{2I_o}{I_{\max} - I_{\min}} \cdot \left( I_{\text{ratio}} - \frac{I_{\max} + I_{\min}}{2I_o} \right). \quad (8)$$

Rewriting Eq. (8) in terms of  $I_{\text{ratio}}$ , it gives:

$$I_{\text{ratio}} = (\text{pH} - \text{p}K_a) \cdot \frac{I_{\max} - I_{\min}}{2I_o} \cdot \frac{1}{2 \cdot b \cdot \log(e)} + \frac{I_{\max} + I_{\min}}{2I_o} = A \cdot \text{pH} + B, \quad (9)$$

where

$$A = \frac{I_{\max} - I_{\min}}{2I_o} \cdot \frac{1}{2 \cdot b \cdot \log(e)},$$

$$B = -\text{p}K_a \cdot \frac{I_{\max} - I_{\min}}{2I_o} \cdot \frac{1}{2 \cdot b \cdot \log(e)} + \frac{I_{\max} + I_{\min}}{2I_o}. \quad (10)$$

### 3 Materials and Methods

The measuring device and the experimental setups have been developed to evaluate the approach under *in vitro* conditions on fresh cow blood and *ex vivo* via monitoring of blood pH in animal models, i.e., a pig and a sheep, undergoing surgery with ECC.

#### 3.1 Optical Transducer and Flow Cuvette

As schematically shown in Fig. 1, the optical transduction of the pH value is based on the fluorescence of a polymeric film directly in contact with the blood flowing in the ECC.

Through an optical head, the fluorescein is excited and the emitted fluorescence signal is collected; finally, a driver, front-end, and signal processing electronics drives the excitation light source and acquires the information of interest.

The polymeric sensing matrix is one of the most important element of the sensor, since it is directly in contact with the blood. So it needs high mechanical strength, but, at the same time, it has to guarantee a fast mass transfer, and in particular

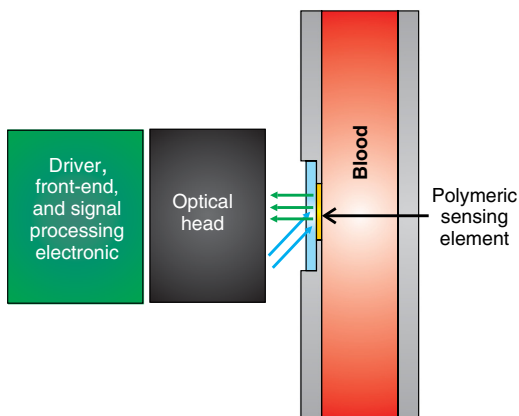


**Fig. 1** Schematic representation of the measurement principle. A polymeric sensing matrix, placed in the flow cuvette directly in contact with the blood, is interrogated by the optical head properly driven by the electronic circuitry.

penetration of hydrogen ions, in order to improve the response time. Finally, it has to be characterized by a low dye leaching. A hydrophilic polymer has been chosen as the matrix, and it has been realized using hydroxyethyl methacrylate (HEMA) which is biocompatible, and it is characterized by a good thermodynamic affinity with water.<sup>28</sup> Moreover, in order to improve the mechanical strength and to avoid a too high swelling, comonomers with functionality four have been added. In particular, a reactive divinyl terminated polyether macromer has been used to increase the chain mobility within the polymer matrix, thus to improve the response time. The fluorescein O-methacrylate 97% is used as the indicator. Since it contains an acrylate group, it is able to covalently link to the polymeric matrix, thus avoiding the dye leaching. The polymeric solution is deposited on polyvinyl chloride (PVC) round substrates and is photopolymerized in an ultra violet (UV)-oven. A picture of the polymeric sensing element, placed in a flow cuvette, is shown in Fig. 2.

The polymeric sensing element is interrogated by an optical head, which has to excite the fluorescein, to collect the fluorescence signal and to monitor the power of the light source. Since the fluorescein O-methacrylate is characterized by an excitation spectrum centered at the wavelength of about  $\lambda_{\text{peak}} = 490$  nm, a blue LED ( $\lambda_{\text{peak}} = 480$  nm) has been used to excite it. Moreover, two photodiodes have been used as photodetectors, one to collect the fluorescence signal and one to monitor the optical power emitted by the LED, thus avoiding the influence of fluctuations of the optical power of the LED. Finally, as usual in fluorescence measurements, two optical filters have been used; in particular, an excitation filter (low-pass filter,  $\lambda_{\text{cutoff}} = 495$  nm) on the light path of the excitation beam and an emission filter (bandpass filter,  $\Delta\lambda = 515 - 535$  nm) on the light path of the fluorescence signal. A schematic representation and a picture of the optical head are shown in Fig. 3.



**Fig. 2** Picture of the polymeric sensing element placed in a flow cuvette.

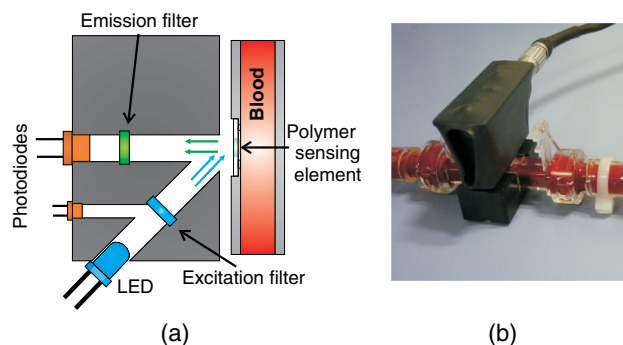


**Fig. 3** Schematic representation (a) and a picture (b) of the optical head. It consists of a blue LED, two photodiodes (to monitor the power emitted by the LED and to collect the fluorescence signal), and finally two optical filters: an excitation filter on the light path of the excitation beam and an emission filter on the light path of the fluorescence emission beam.

### 3.2 Driving Electronics and Analog Signal Processing Circuitry

The operation of the measuring device is based on the electronic circuitry for exciting the blue LED and conditioning the signals provided at the photodiode detectors output. According to our previous paper,<sup>21</sup> the blue LED is excited by current pulses (duration 800 ms) at a frequency of 0.125 Hz. During the pulse the current was modulated sinusoidally at a frequency of 6.06 kHz. This double modulation allows us to reduce the effects of photobleaching<sup>21</sup> and improve the signal-to-noise ratio operating a proper demodulation of the photodetectors output. The front-end electronics consists in two channels devoted to the processing of the monitor and fluorescence photogenerated current signals. Each channel includes: (1) a low-noise trans-impedance preamplifier; (2) a high-Q bandpass filter with center frequency at 6.06 kHz; (3) a lock-in amplifier; (4) a lowpass filter with a 70-Hz passband cutoff, and (5) an analog-to-digital converter. Figure 4 shows the block diagram of the electronics and two pictures of the measuring system including the optical head.

### 3.3 Regression Model

$I_{ratio}$  has been estimated by the voltage ratio,  $V_{ratio}$ , between the signals generated by the front-end electronics, i.e.,  $V_{fluor}$  and  $V_{mon}$ . Since the proportionality coefficient between  $V_{ratio}$  and

$I_{ratio}$  and parameters  $A$  and  $B$  in Eq. (9) are unknown, the relationship between pH and  $V_{ratio}$  was determined using a linear regression model. Starting from Eq. (9), we introduced two regression coefficients  $\tilde{A}$  and  $\tilde{B}$  calculated through a least squares method relating the values of  $V_{ratio}$  and the actual pH values measured by the blood gas analyzer according to the regression model:

$$V_{ratio} = \tilde{A} \cdot pH + \tilde{B}. \quad (11)$$

This linear approximation is considered to be valid in the pH range of interest (RoI) (6.9 to 8).

### 3.4 Experimental Protocol for In Vitro Test

Figure 5 shows the mock system assembled to simulate the blood condition during ECC. It consists of: (1) a centrifugal pump, capable of guaranteeing a flux up to 6 L/min; (2) a heat exchanger based on the Peltier effect (temperature ranging 15°C to 39°C); (3) an oxygenator; and (4) an arterial/venous bubble filter. The whole circuit volume, including the centrifugal pump, the heat exchanger, the oxygenator, the arterial-venous bubble filter and the tubing set is 760 ml. The flow cuvette was positioned in the tubing connecting the filter and the reservoir, on the arterial line. The optical probe was fixed to the flow cuvette according to the setup shown in Fig. 3, and the fluorescence and monitor signals were collected and

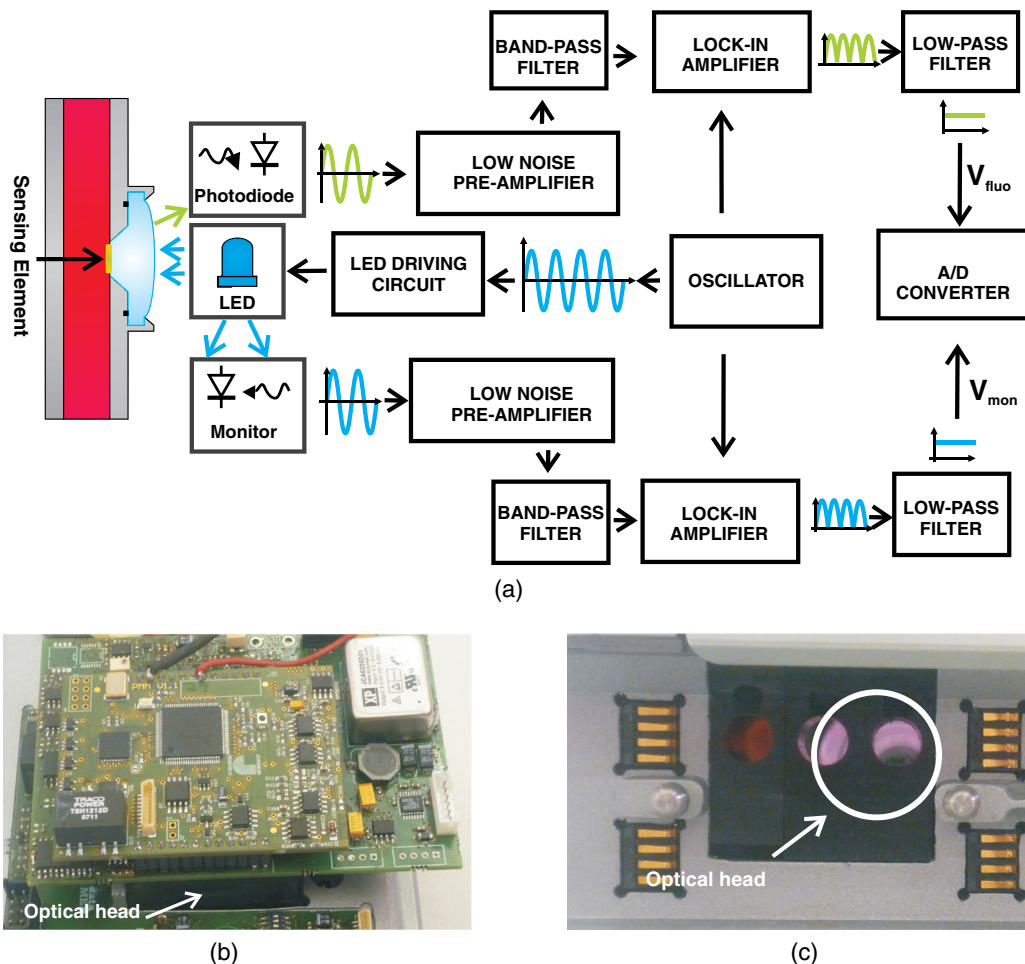
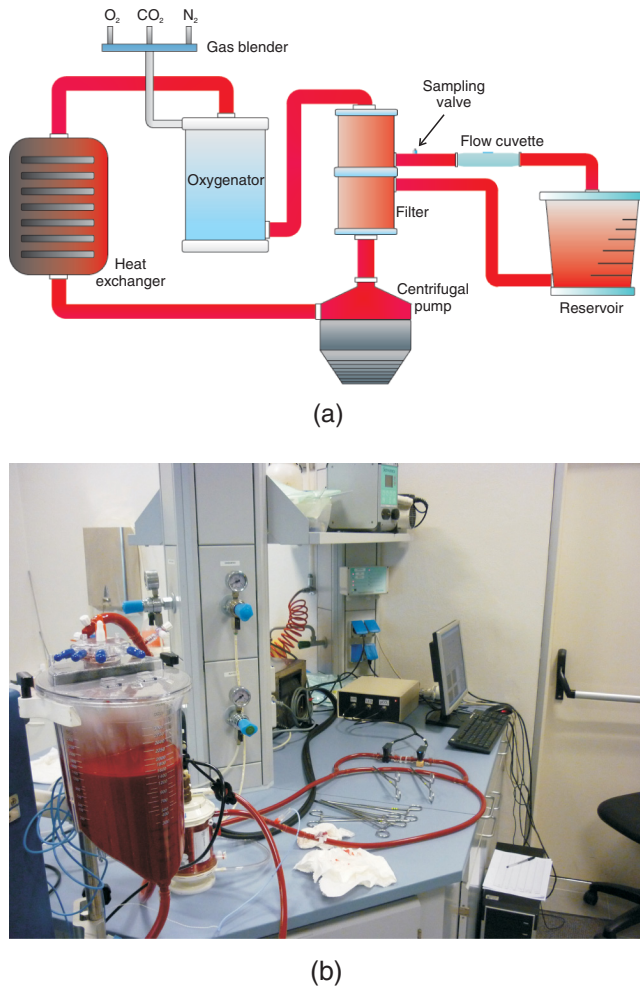


Fig. 4 Block diagram of the electronics (a) and pictures of the measuring system including the optical head, back view (b) and front view (c).



**Fig. 5** Block diagram (a) and picture (b) of the mock system realized to simulate the blood condition during ECC. It consists of a centrifugal pump, an oxygenator, a heat exchanger, an arterial/venous bubble filter, a sampling valve, a flow cuvette, and tubings.

analyzed by the front-end electronics that generates  $V_{ratio}$ . A constant blood flow (2 L/min) was maintained throughout the experiments. Blood samples were obtained from the extracorporeal line close to the flow cuvette (sampling valve). The protocol described above was repeated for two different blood temperatures, 37°C and 32°C, since frequently in cardiac surgery a moderate hypothermia condition is induced. The dependence of the sensor on the blood saturation was not investigated, since it is correlated with the variation of pH.

The cow was exsanguinated at local slaughterhouse 1 h before the experiment. The collected blood was stored in heparinized container at 4°C during the transportation. Whole blood is an intrinsically complex fluid and difficult to manipulate, thus great care was devoted to not alterate natural condition of the sample. Before the experiment, the blood was diluted with saline solution and used to fill the reservoir with 3 L of fluid. The hemodilution was adjusted to provide sample with a hematocrit of 33% to 34%. The values of partial pressure of oxygen ( $pO_2$ ), carbon dioxide ( $pCO_2$ ), and pH were adjusted to normal physiological range previous the measurement session. All blood gas analyses were performed with a commercial blood gas analyzer (ABL, Radiometer A/S, Copenhagen, Denmark).

### 3.5 Experimental Protocol for Ex Vivo Test

The study was approved by the the Animal Care Ethical Committee of the University of Modena and Reggio Emilia. The experiments followed the recommendations described in the Italian law (D.L. 27-1-1992 n. 116). A veterinary doctor was constantly involved in the activities to control animals wellness and health. First experiment was performed on an adult female pig (see note, Table 1). To confirm the results obtained during this experiment a second sensor has been tested on an adult female sheep (see note, Table 2).

During each surgery the sensor (different sensing elements have been used in the two experiments) was attached to the arterial line of the ECC circuit. A total of 20 samples were analyzed by a blood gas analyzer (ABL, Radiometer A/S, Copenhagen, Denmark) during the two surgeries with pH varying in the range 7.2 and 7.5. The experimental setup for *ex vivo* evaluation of the measuring system is shown in Fig. 6. It consists of the standard ECC setup including the flow cuvette placed between the animal and the arterial filter.

The following blood parameters were monitored during the experiment: blood flow rate by flow probes (H9XL Flow Probe, Transonic Systems Inc., Artisan Sci. Co., Champaign, Illinois), blood pressures by digital sensors (DPI 705, Druck Ltd, Leicester, England), blood temperatures by thermistor probes (Exacon® Medical Temperature Probe, Exacon Scientific A/S, Roskilde, Denmark) and digital thermometer (Omega HH41, Engineering Inc., Stamford, Connecticut), blood gases ( $p_aO_2$ : oxygen partial pressure in the arterial blood;  $p_vO_2$ : oxygen partial pressure in the venous blood;  $p_aCO_2$ : carbon dioxide partial pressure in the arterial blood;  $S_aO_2$ : hemoglobin oxygen saturation in the arterial blood) by a blood gas analyzer (ABL, Radiometer A/S, Copenhagen, Denmark); hematocrit by a HCT minicentrifuge (Hematocrit Centrifugette 4203, ALC International S.r.L., Cologno Monzese, Milan, Italy), blood electrolytes and activated clotting time (ACT) (ACT Plus™, Medtronic Perfusion Systems, Minneapolis, Minnesota). Heparin was

**Table 1** Details of the pig involved in the *ex vivo* experiment.

Race: Large white (Female)	Weight: 80 kg
Sedation	Zolazepam (Zoletil®) 5 mg/kg + Atropine 1 ml
Induction	Propofol
Maintenance	Isoflurane + O <sub>2</sub>
Analgesia	Morphine + 0.3 mg/kg

**Table 2** Details of the sheep involved in the *ex vivo* experiment.

Sheep (Female)	Weight: 55 kg
Sedation	Tiletamine and Zolazepam (Zoletil®) + Atropine 0.66 mg/kg
Induction	Propofol
Maintenance	Fentanyl 0.1 mg/kg + Propofol 22.5 mg/kg + 2% isoflurane in 50% N <sub>2</sub> O/50% O <sub>2</sub>

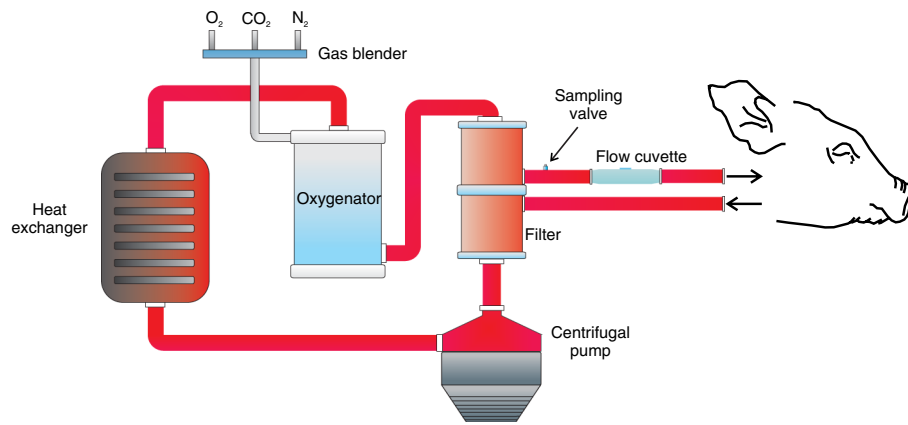


**Fig. 6** Block diagram of the experimental setup for *ex vivo* evaluation of the measuring system.



**Fig. 7** Pictures of the environment test during the experiment performed on the pig (a) and sheep (b).

continuously infused during the experiment in order to keep the ACT between 300 s and 450 s. The pig was perfused for 9 h in venous-arterial mode (iliac artery and vein were cannulated by two bypass cannulas), in normothermic condition (37.5°C to 38°C). The sheep was perfused for 11 h in venous-arterial mode (right carotid artery and jugular vein were cannulated by two bypass cannulas), under controlled hypothermia (33.2°C and 34.5°C). The pH of blood was sampled with a time interval of 1 h in each *ex vivo* experiment, obtaining nine samples in the *ex vivo* experiment on the pig and 11 on the sheep. The pictures of the environment test during the two *ex vivo* experiments are shown in Fig. 7.

## 4 Results

### 4.1 In Vitro Experimental Results

In Fig. 8,  $V_{\text{ratio}}$  versus time is shown, for a measurement performed on cow blood, changing the pH of the blood. The dots are the average values of the  $V_{\text{ratio}}$  signal recorded at each reference pH (diamonds), measured by the blood gas analyzer. During this test, both the flow rate and the temperature of blood were kept constant, at a value of 2 L/min and 37°C, respectively. The pH of the blood was changed using gases, in particular carbon dioxide and nitrogen. The oxygen was kept quite constant, thus the saturation was always above 90%. The hematocrit of the blood was always kept at a value of 33% to 34%.

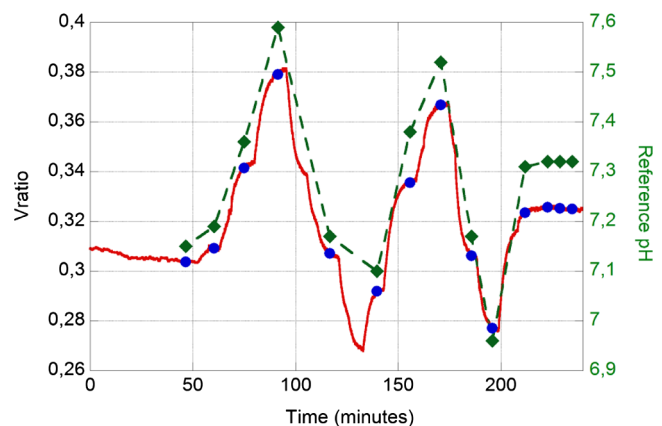


**Fig. 8**  $V_{\text{ratio}}$  versus time measured *in vitro*, changing the pH of the blood. The dots are the average values of the  $V_{\text{ratio}}$  signal recorded at each reference pH (diamonds), measured by the blood gas analyzer.

**Table 3** Coefficients  $\tilde{A}$  and  $\tilde{B}$  of the regression model and correlation index, determined considering the mean values of the  $V_{\text{ratio}}$  (averaged over a time interval of 60 s).

$\tilde{A}$	0.1628
$\tilde{B}$	-0.8615
$R$	0.9887

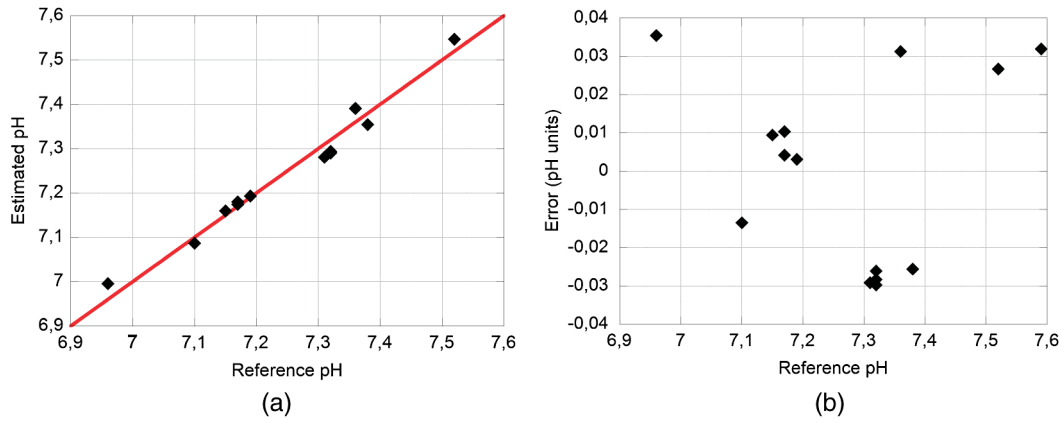


**Fig. 9** Estimated pH versus reference pH and the interpolation line (a). The interpolation line was obtained by applying the regression model on the mean values of the  $V_{ratio}$ , calculated over an interval of 60 s, at every reference pH value. Difference between the estimated pH and the reference pH, versus the reference pH (b).

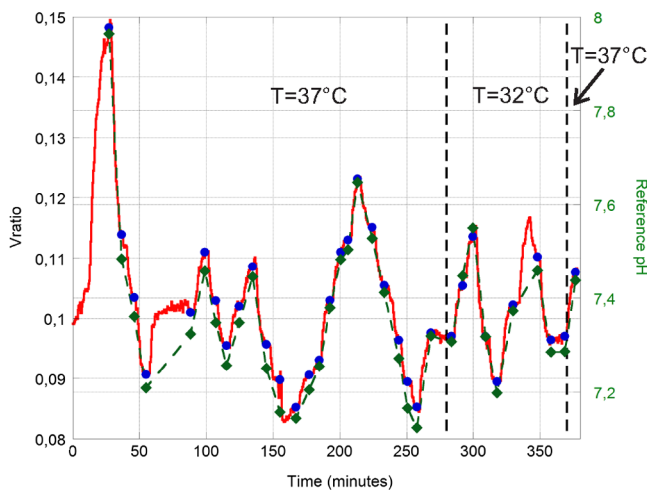


**Fig. 10**  $V_{ratio}$  versus time measured during an *in vitro* experiment. The dots are the average values of the  $V_{ratio}$  signal measured at each reference pH (diamonds). To investigate the potential influence of a moderate ipothermia condition on the recorded signal, the temperature was initially kept at a value of 37°C, then was brought to 32°C (between the two black vertical dashed lines), and finally changed back to 37°C.

The data interpolation was obtained by applying the regression model on the mean values of  $V_{ratio}$ , calculated over a time interval of 60 s, at each reference pH value. The coefficients  $\tilde{A}$ ,  $\tilde{B}$  and the correlation index determined by the regression model are reported in Table 3.

The linearity and the difference between the pH measured by our system and the pH determined by the blood gas analyzer are shown in Fig. 9.

The mean square error value, calculated as:

$$\epsilon = \sqrt{\frac{\sum_i (\text{pH}_{\text{Measured}_i} - \text{pH}_{\text{Estimated}_i})^2}{N}}, \quad (12)$$

was determined to be 0.0243 units of pH (2.2% of the RoI).

Frequently in cardiac surgery a moderate ipothermia condition is induced. To investigate the potential influence of this procedure on the recorded signal, measurements were performed varying the temperature from 37°C to 32°C. During this test, the temperature was initially kept at a value of 37°C, then

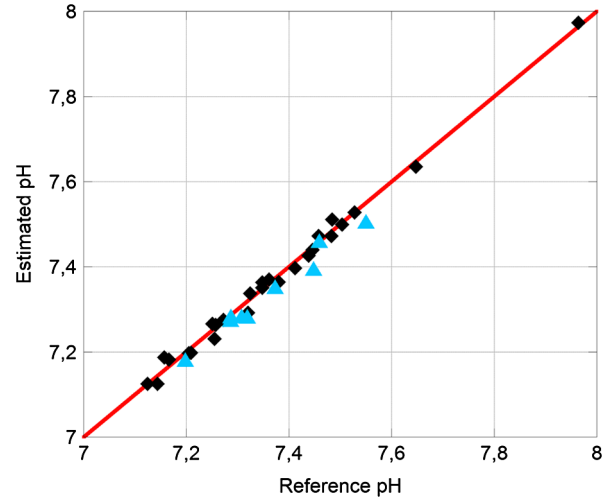


**Fig. 11** Estimated pH versus reference pH and the interpolation line, obtained by applying the regression model on the mean values of the  $V_{ratio}$  recorded at 37°C. The diamonds are the data acquired at 37°C, whereas the triangles were measured at 32°C.

was brought to 32 °C, and finally changed back to 37°C. In Fig. 10,  $V_{ratio}$  versus time is shown; during the time period included between the two black vertical dashed lines the temperature was brought to 32°C. The dots are the average values of the  $V_{ratio}$  signal measured at each reference pH (diamonds).

Results of the regression method, calculated considering only the pH measured at 37°C, applied to the mean values of the  $V_{ratio}$  (averaged over a time interval of 60 s) are shown in Fig. 11. The diamonds are the reference pH measured at 37°C, whereas the triangles were measured at 32°C.

**Table 4** Coefficients  $\tilde{A}$  and  $\tilde{B}$  of the regression model and correlation index, determined considering the mean values of the  $V_{ratio}$  (averaged over a time interval of 60 s) of the pH recorded at 37°C.

$\tilde{A}$	0.0743
$\tilde{B}$	-0.4440
$R$	0.9936

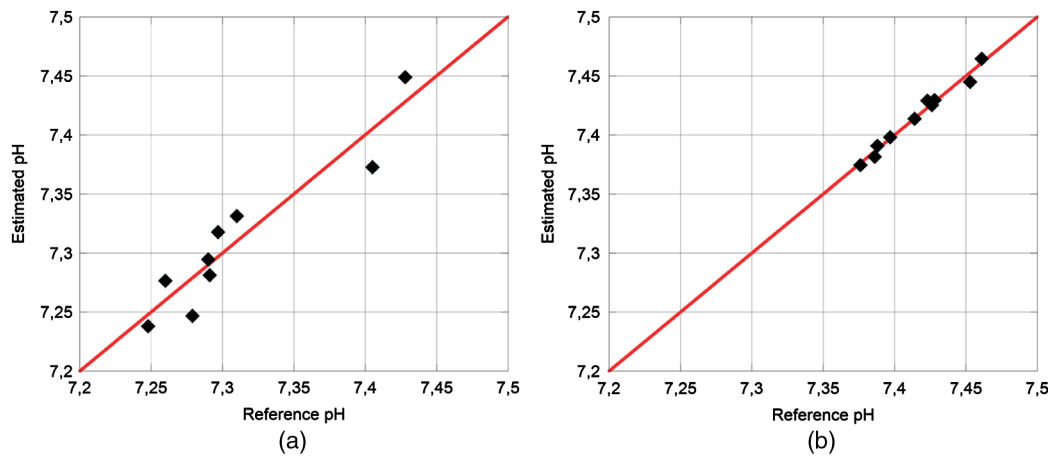


**Fig. 12** Estimated pH measured by our system versus reference pH determined by the commercial blood gas analyzer and the interpolation line, measured in the *ex vivo* tests performed on the pig (a) and on the sheep (b).

**Table 5** Coefficients  $\tilde{A}$  and  $\tilde{B}$  of the regression model and correlation index, determined considering the mean values of the  $V_{\text{ratio}}$  (averaged over a time interval of 60 s) in the *ex vivo* experiments on a pig and on a sheep.

	Pig	Sheep
$\tilde{A}$	0.1213	0.4889
$\tilde{B}$	-0.6541	-3.516
$R$	0.9431	0.9901

The coefficients  $\tilde{A}$ ,  $\tilde{B}$ , and the correlation index determined by the regression model are reported in Table 4.

The mean square errors, calculated according to Eq. (12), were 0.0150 units of pH for the acquisition at 37°C (1.3% of the RoI) and 0.0280 for the acquisition at 32°C (2.5% of the RoI).

#### 4.2 Ex Vivo Experimental Results

In *ex vivo* experiments, the pH was changed only with little variations, thus avoiding to compromise the physiological functions of the animals. The linearity between the pH measured by our system and the pH determined by the commercial blood gas analyzer is shown in Fig. 12. The coefficients  $\tilde{A}$ ,  $\tilde{B}$ , and the correlation index determined by the regression model are reported in Table 5.

The mean error was determined to be 0.0038 units of pH (0.3% of the RoI) for the experiment performed on the sheep and 0.0208 units of pH (1.9% of the RoI) for the one performed on the pig.

### 5 Discussion and Conclusions

Intermittent sampling of blood and the consequent delay between blood withdraw and pH data availability to medical staff can represent a critical aspect, especially during unexpected conditions that might happen during ECC. In this paper, we present a high correlation ( $R$  of 0.9887 and 0.9936 *in vitro* and  $R$  of 0.9431 and 0.9901 *ex vivo*) between pH value determined

by our device and pH measured by a commercial blood gas analyzer during *in vitro* and *ex vivo* experiments.

The proposed measuring system that includes a biocompatible film in contact with blood, generated accurate and consistent measurements of blood pH during *in vitro* and *ex vivo* experiments. The continuous and real-time characteristics of the haematic pH sensor described in this article may improve the safety of patient management during ECC. The obtained results demonstrate the possibility of monitoring pH in real-time during ECC using a disposable sensing element based on the fluoresceine O-methacrylate 97%, included in a crosslinked polymer matrix. Dye leaching is minimized by the covalent link between the fluorophore and polymer matrix, nevertheless, even in presence of minimal leaching due to a not complete reaction of fluoresceine O-methacrylate this fluorophore is absolutely biocompatible and not toxic for the patient.

After calibration, we found a mean square error lower than the 3% of the RoI both for *in vitro* and *ex vivo* measurements. Considering an ipothermic treatment at 32°C, the mean square error, calculated with the calibration curve obtained considering only the pH values recorded at 37°C, was lower than 3% of the measuring range. This means that this sensor is suitable for ipothermic treatment without the need of a new calibration curve.

However, a different set of calibration coefficients was obtained for each sensing element. This variation is mainly associated to the reproducibility of the deposition of the polymer film on the substrate. Therefore a calibration procedure before each ECC treatment is required. This might be problematic, since at least two points of calibration are required. This procedure leads to two main disadvantages: (1) a commercial blood gas analyzer is always required in order to calibrate the sensor (limiting its field of application); (2) calibrating the sensor on a human being may be difficult since, in normal conditions, pH has little variations. This means that the sensor is likely to be calibrated with two near points, with a high probability of committing a big error for pH values out of the range of calibration. These problems could be overcome calibrating the sensor with two buffer physiological solutions with an already-known pH. Nevertheless, this approach could be problematic for perfusionists who are accustomed to use only one priming physiological solution.

The developed system is not right away suitable for clinical applications. For this reason, future work will look at the

fabrication of the sensing element to improve the repeatability of the sensors response. In this way, it will be possible to calibrate some sample sensors of the same production lot before the use on ECC and then using the same calibration curve for all the sensors of the lot. Thus it could be possible to use a generic sensor on ECC just taking a point of calibration, in order to adjust the calibration offset. Moreover, we are considering to extend the proposed approach to the measurement of other blood parameters of interest in ECC, providing the basis for a multi-analyte blood gas sensor.<sup>29,30</sup> This exciting development could lead to a new valuable clinical sensing tool for continuous monitoring of blood in ECC.

### Acknowledgments

This work was partially funded by RanD S.r.l., Medolla, Modena.

### References

1. D. Schneditz et al., eds., "Extracorporeal Sensing Techniques in Cardiovascular Disorders in Hemodialysis," *Contrib. Nephrol., Karger* **149**(1), 35–41 (2005).
2. J. Tusa and H. He, "Critical care analyzer with fluorescent optical chemosensors for blood analytes," *J. Mater. Chem.* **15**(27–28), 2640–2647 (2005).
3. A. Pesatori, M. Norgia, and L. Rovati, "Self-mixing laser doppler spectra of extracorporeal blood flow: a theoretical and experimental study," *IEEE Sens. J.* **12**(3), 552–557 (2012).
4. A. Pesatori, M. Norgia, and L. Rovati, "Low-cost optical flowmeter with analog front-end electronics for blood extracorporeal circulators," *IEEE Trans. Instrum. Meas.* **59**(5), 1233–1239 (2010).
5. M. Ushizima, S. Muuhlen, and I. Cestari, "A low-cost transmittance transducer for measurement of blood oxygen saturation in extracorporeal circuits," *IEEE Trans. Biomed. Eng.* **48**(4), 495–499 (2001).
6. D. Myklejord et al., "Clinical evaluation of the on-line sensicath™ blood gas monitoring system," *Heart Surg. Forum* **1**(1), 60–64 (1998).
7. S. Perov et al., "Principles of optical oximetry in extracorporeal circulation systems," *Biomed. Eng.* **26**(5), 243–247 (1992).
8. F. Gamero, M. Ushizima, and I. Cestari, "Real time monitoring of oxygen saturation in extracorporeal circulation using an optical reflectance transducer," *Artif. Organs* **25**(11), 890–894 (2001).
9. J. Jiang et al., "Development of fiber optic fluorescence oxygen sensor in both *in vitro* and *in vivo* systems," *Respir. Physiol. Neurobiol.* **161**(2), 160–166 (2008).
10. C. Morgan et al., "Continuous neonatal blood gas monitoring using a multiparameter intra-arterial sensor," *Arch. Dis. Child. Fetal Neonatal Ed.* **80**(2), F93–F98 (1999).
11. M. Ganter and A. Zollinger, "Continuous intravascular blood gas monitoring: development, current techniques, and clinical use of a commercial device," *Br. J. Anaesth.* **91**(3), 397–407 (2003).
12. H. Endoh et al., "Continuous intra-jugular venous blood-gas monitoring with the Paratrend 7 during hypothermic cardiopulmonary bypass," *Br. J. Anaesth.* **87**(2), 223–228 (2001).
13. S. Marxer and M. Schoenfisch, "Sol-gel derived potentiometric pH sensors," *Anal. Chem.* **77**(3), 848–853 (2005).
14. Z. Liu, J. Liu, and T. Chen, "Phenol red immobilized PVA membrane for an optical pH sensor with two determination ranges and long-term stability," *Sensor. Actuat. B Chem.* **107**(1), 311–316 (2005).
15. P. Hashemi and R. Zarjani, "A wide range pH optical sensor with mixture of neutral red and thionin immobilized on an agarose film coated glass slide," *Sensor. Actuat. B Chem.* **135**(1), 112–115 (2008).
16. L. Rovati et al., "Construction and evaluation of a disposable pH sensor based on a large core plastic optical fiber," *Rev. Sci. Instrum.* **82**(2), 023106 (2011).
17. D. Wencel, B. MacCraith, and C. McDonagh, "High performance optical ratiometric sol-gel based pH sensor," *Sensor. Actuat. B Chem.* **139**(1), 208–213 (2009).
18. Z. Li et al., "A novel fluorescence ratiometric pH sensor based on covalently immobilized piperaziny-1,8-naphthalimide and benzothioxanthene," *Sensor. Actuat. B Chem.* **114**(1), 308–315 (2006).
19. I. Sánchez-Barragán et al., "A ratiometric approach for pH optosensing with a single fluorophore indicator," *Analytica Chimica Acta* **562**(2), 197–203 (2006).
20. L. Ferrari et al., "Haematic pH sensor for extracorporeal circulation," *Proc. SPIE* **8214**, 82140E (2012).
21. L. Ferrari et al., "Photobleaching effects in organic thin film sensing probes," in *IEEE Int. Instrumentation and Measurement Technology Conf.*, pp. 1235–1239, IEEE, Graz, Austria (2012).
22. Y. Kostov and G. Rao, "Low-cost optical instrumentation for biomedical measurements," *Rev. Sci. Instrum.* **71**(12), 4361–4374 (2000).
23. I. Johnson and M. T. Z. Spence, *Molecular Probes Handbook, A Guide to Fluorescent Probes and Labeling Technologies*, 11th ed., Life Technologies, Invitrogen, Carlsbad, California (2010).
24. J. K. Tusa and M. J. P. Leiner, "Optodes fluorescentes pour analytes de l'urgence," *Annales de Biologie Clinique* **61**(2), 183–191 (2002).
25. Y. A. Povrozin et al., "Near-infrared, dual-ratiometric fluorescent label for measurement of pH," *Anal. Biochem.* **390**(2), 136–140 (2009).
26. A. S. Vasylevska et al., "Novel coumarin-based fluorescent pH indicators, probes and membranes covering a broad pH range," *Anal. Bioanal. Chem.* **387**(6), 2131–2141 (2007).
27. E. Braunwald et al., *Harrison's Principles of internal medicine*, McGraw Hill, New York City (2002).
28. L. Li and L. J. Lee, "Photopolymerization of HEMA/DEGDMA hydrogels in solution," *Polymer* **46**(25), 11540–11547 (2005).
29. N. Joglekar et al., "A review of blood gas sensors and a proposed portable solution," in *Int. Symposium on Integrated Circuits*, pp. 244–247, IEEE, Singapore (2007).
30. C. Cooney and B. Towe, "Evaluation of microfluidic blood gas sensors that combine microdialysis and optical monitoring," *Med. Biol. Eng. Comput.* **42**(5), 720–724 (2004).